

Spindle cell/sclerosing rhabdomyosarcoma with intracranial invasion without destroying the bone of the skull base: a case report and literature review

Daichi Momosaka¹, Osamu Togao¹, Akio Hiwatashi¹,
Koji Yamashita¹, Koji Yoshimoto², Megumu Mori², Toru Iwaki³
and Hiroshi Honda¹

Abstract

Spindle cell/sclerosing rhabdomyosarcoma (ssRMS) is a new subtype of rhabdomyosarcoma included in the World Health Organization soft tissue and bone tumor classification in 2013. Despite the increasing number of reported cases of ssRMS, the imaging characteristics of ssRMS are not established. Herein, we present the case of an elderly Japanese woman with ssRMS of the masticator space with intracranial invasion without destruction of the adjacent bone. Attention should be paid to the presence of intracranial infiltration that may indicate a worse prognosis. Tumor growth without bone destruction could be a key finding to differentiate ssRMSs from conventional subtypes of rhabdomyosarcoma.

Keywords

Soft-tissue neoplasms, head and neck neoplasms, rhabdomyosarcoma, multi-detector computed tomography, magnetic resonance imaging (MRI)

Date received: 2 June 2017; accepted: 29 July 2017

Introduction

Rhabdomyosarcoma (RMS) is a rare and aggressive malignancy that may originate from primitive mesenchymal cells that arise anywhere in the body, including sites where striate muscle is not found (1). RMSs are common in children, representing 5% of all childhood cancers (2). RMSs are rare in adults; soft-tissue sarcomas make up fewer than 1% of malignancies in adults and RMS make up only 3% of all soft-tissue sarcomas (3). RMSs were traditionally classified into three main subtypes: embryonal; alveolar; and pleomorphic. Imaging findings of these conventional subtypes of RMSs are variable and non-specific; solitary unilateral bulky lesions showing either extremely low, high or intermediate signal intensities compared to muscles on T2-weighted (T2W) images, and moderate contrast enhancement with non-enhancing areas representing central necrosis or cavitation (1).

However, additional variants were identified, including spindle cell RMS and sclerosing RMS (ssRMS); these were added as a new subtype in the latest classification of diseases of the World Health Organization (WHO) (4).

Despite the increasing number of reported cases of ssRMS (5–35), little is known about its radiological

¹Department of Clinical Radiology, Graduate School of Medical Sciences, Kyushu University, Fukuoka, Japan

²Department of Neurosurgery, Graduate School of Medical Sciences, Kyushu University, Fukuoka, Japan

³Department of Neuropathology, Graduate School of Medical Sciences, Kyushu University, Fukuoka, Japan

Corresponding author:

Daichi Momosaka, Department of Clinical Radiology, Graduate School of Medical Sciences, Kyushu University, 3-1-1 Maidashi, Higashi-ku, Fukuoka 812-8582, Japan.

Email: dmomosaka@icloud.com



findings. Herein, we present a case of ssRMS in the masticator space with an intracranial invasion without destruction of the adjacent bone of the skull base. We also compare the radiological findings of ssRMS with those of conventional subtypes of RMS.

Case report

A 67-year-old Japanese woman visited our hospital with swelling of the right temporal region that had been present for the prior three weeks and left-sided hemiparesis for the prior one week. The patient had no history of medication or surgical intervention. The results of routine laboratory tests were normal. On computed tomography (CT), the right temporal mass consisted of two components; an extracranial component in the right masticator space and an intracranial component in the right middle cranial fossa (Fig. 1a). The skull base sandwiched by the two components of the mass was not destroyed, but rather showed sclerosis and thickening (Fig. 1b).

On magnetic resonance imaging (MRI), the extracranial component showed homogeneous high intensity on T2W (Fig. 2a) and iso-intensity on T1-weighted (T1W) images compared to that in the muscle. The intracranial component showed heterogeneous high intensity on T2W (Fig. 2b) and T1W images (Fig. 2c). Many flow voids were seen within the mass. On diffusion-weighted imaging (DWI), the solid area showed mild high intensity (Fig. 2d). The minimum apparent diffusion coefficient (ADC) of the solid area was $0.88 \times 10^{-3} \text{ mm}^2/\text{s}$.

On coronal contrast-enhanced fat-suppressed T1W images, the mass showed homogenous contrast enhancement in the extracranial component, whereas it showed heterogeneous enhancement in the

intracranial component. The extracranial and intracranial components communicated via the foramen ovale (Fig. 2e). Magnetic resonance angiography (MRA) showed that many branches of the right external carotid arteries (branches from deep temporal artery and middle meningeal artery) were distributed in the tumor (Fig. 2f). Perfusion-weighted images showed elevated blood flow and blood volume in the tumor.

As the intracranial component of the mass caused compression and distortion of the brainstem, which threatened the life of the patient, emergency surgery was performed and the intracranial component of the mass was resected. The tumor was fibrous and severely adhered to the dura of the temporal base, although the margin between the tumor and temporal lobe was clear. Intraoperative findings proved the intracranial tumor component was connected to the extracranial component through the foramen ovale.

The histopathologic analysis showed the tumor consisted of interlacing, fascicular proliferated spindle-shaped tumor cells and fibrocollagenous stroma (Fig. 3a). Rhabdomyoblast-like cells with cellular atypia were occasionally observed (Fig. 3b). Bone invasion of the tumor cells was identified. Dilated blood vessels, necrotic changes, and hemorrhages were frequently seen. On immunohistochemistry, the tumor cells were positive for desmin (Fig. 3c), myogenin (Fig. 3d), and vimentin, but negative for caldesmon and CD34. The Ki-67 labeling index was 36.6%. In conjunction with the histological and immunohistochemical findings, the tumor was diagnosed as ssRMS.

The patient's symptoms were relieved after the surgery and no additional treatments were performed. The patient died of an intracranial recurrence of the tumor at approximately three months after the surgery.

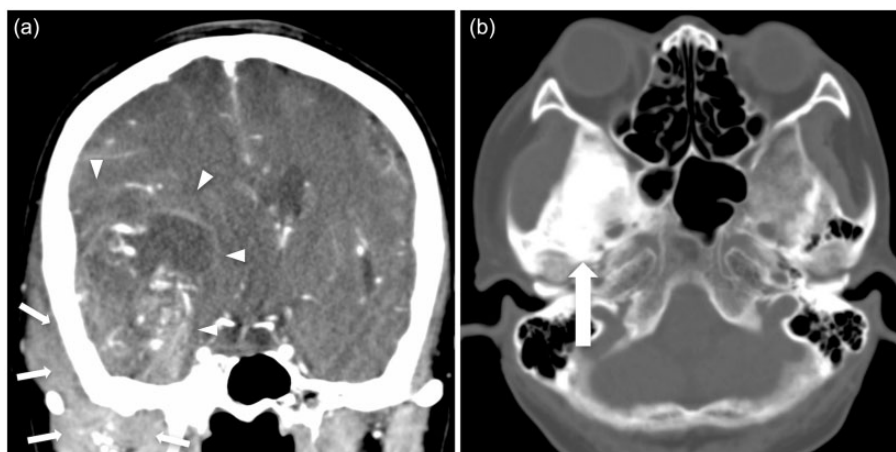


Fig. 1. Coronal contrast-enhanced CT images showed that the mass consisted of two components; the extracranial component in the right masticator space (a; arrows) and the intracranial component in the right middle cranial fossa (a; arrowheads). The floor of the right middle cranial fossa showed bone sclerosis and thickening (b; arrow).

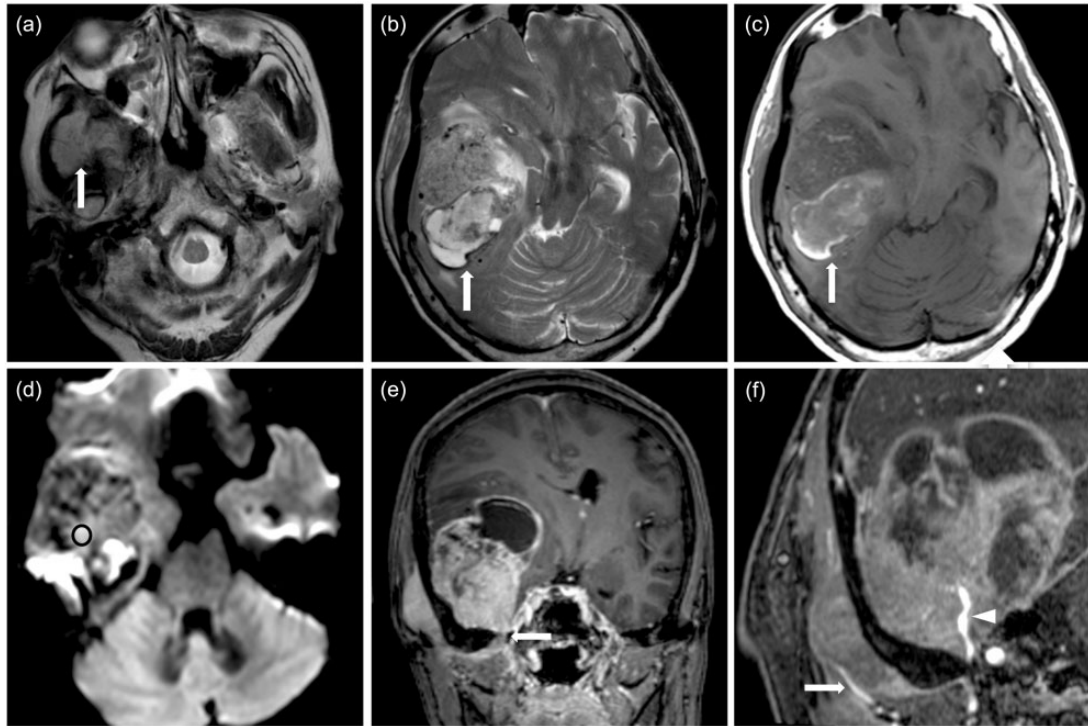


Fig. 2. On axial T2W images, the extracranial component of the mass showed homogeneous mildly high intensity (a; arrow) compared to the muscles, and the intracranial component showed heterogeneous intensity (b; arrow) suggesting intratumoral necrotic or cystic changes. On axial T1W images, the intracranial component of the mass partially demonstrated high intensity (c; arrow) representing intratumoral hemorrhaging. On DWI obtained with $b = 1000 \text{ s/mm}^2$, the solid area of the mass showed slightly high intensity (d; circle). The ADC value of the same area was $0.88 \times 10^{-3} \text{ mm}^2/\text{s}$. On coronal contrast-enhanced fat-suppressed T1W images, the extracranial and intracranial components of the mass demonstrated heterogeneous and strong contrast enhancement. The coronal section through the foramen ovale shows the two components communicated with each other via the foramen ovale (e; arrow). On oblique MRA images, the extracranial component of the mass was fed by the deep temporal artery (f; arrow). The intracranial component of the mass was fed by the middle meningeal artery (f; arrowhead).

Discussion

Our literature search identified 163 reported cases of ssRMS (5–35). The key epidemiologic features of ssRMS are summarized in Fig. 4a and b. Although ssRMSs have been reported in all age groups (<1–79 years), 57% of the cases were detected in adults (>18 years). There was a mild predilection for boys/men (60%). Approximately one-third of the cases occurred in the head and neck region. However, to the best of our knowledge, the present case is the first case of ssRMS in the masticator space with intracranial invasion.

Although the masticator space is a predilection site of ssRMS, there have been no reports of ssRMS cases originating from intracranial tissues. Additionally, in the present case both the intra- and extra-cranial components were fed by branches of the external carotid arteries. These features suggested that the ssRMS of our patient arose primarily from the masticator space and extended into the middle cranial fossa via the foramen ovale. Interestingly, the intracranial component showed more heterogeneous intensity on T1W and

T2W images compared to the extracranial component, suggesting intratumoral hemorrhaging and necrotic changes. These changes might represent a rapid and aggressive alteration in the intracranial component, but not in the extracranial component.

It has been reported that the conventional subtypes of RMS in parameningeal locations (such as the nasopharynx, the parapharyngeal space, the masticator space, the nasal cavity, paranasal sinuses, the mastoid, and the middle ear) could spread to the skull base or intracranial area, and this finding was related to worse prognoses (1). The details of the present case indicate that ssRMSs can also show intracranial invasion. Clinicians should note this finding because it may lead to a poorer prognosis, as in the conventional subtypes.

In our patient's case, there was no lytic lesion in the skull base, but there was sclerosis and thickening of the bones. This finding is consistent with previous reports of ssRMS (14,22,27). This growth pattern without bone destruction may be a key finding to differentiate ssRMSs from the conventional subtypes of RMS,

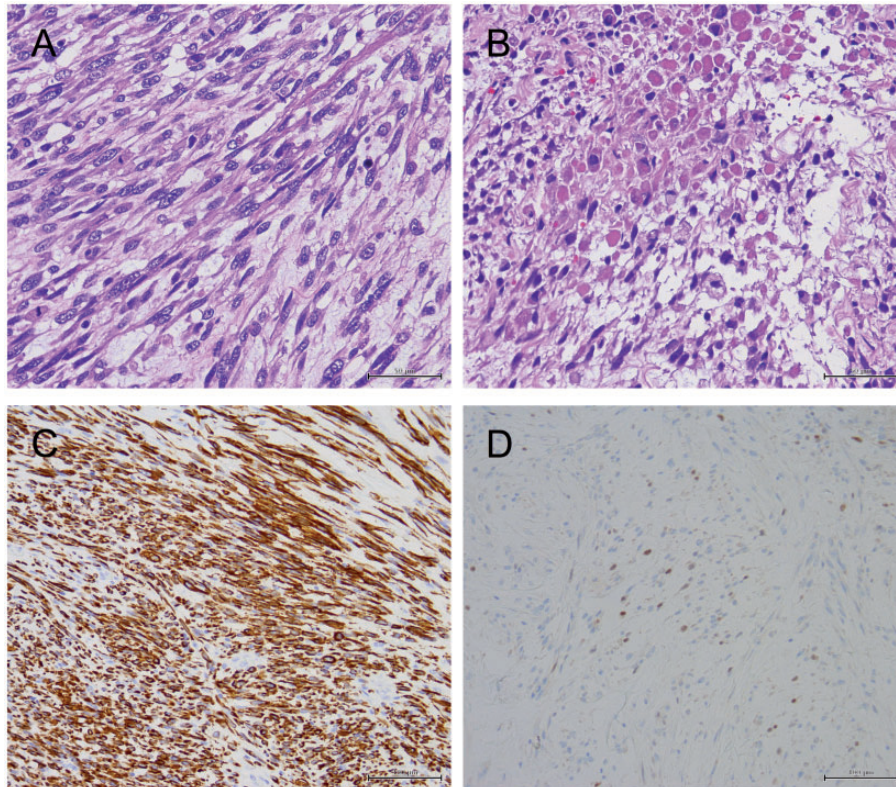


Fig. 3. Hematoxylin and eosin (H&E) stain ($\times 400$ magnification) section showed that the tumor consisted of interlacing, fascicular proliferated spindle-shaped tumor cells and fibrocollagenous stroma (a). Rhabdomyoblast-like cells with cellular atypia were occasionally observed (b). On immunohistochemistry, desmin (c) and myogenin (d) were positive.

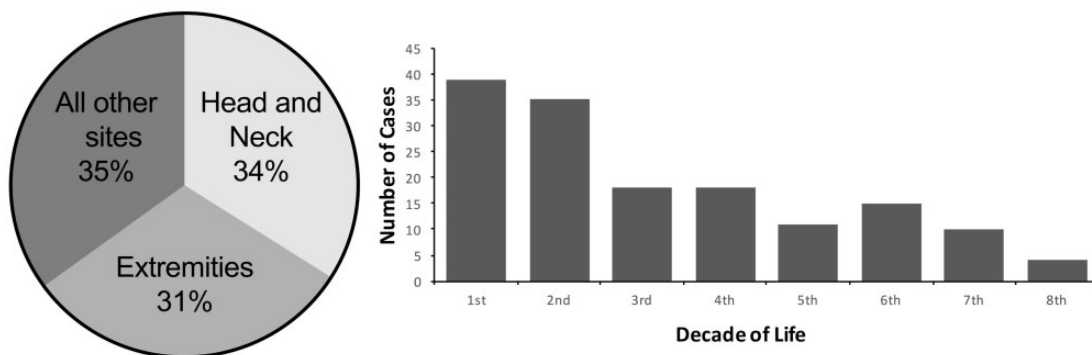


Fig. 4. Site distribution of ssRMS in previously published cases (a). Head and neck and extremities are the most common sites of ssRMS. Age distribution (by decade) of SSRMS in the published cases (b). ssRMSs are diagnosed in a wide age range.

which tend to show the destruction of adjacent bones (36).

There are only ten case reports of ssRMS showing radiological findings or images of ssRMS (10,14,21–24,27,28,30,34). These are summarized in Table 1. In most cases, ssRMSs show mildly high intensity on T2W and iso-intensity on T1W images compared to the muscles. On post-contrast images, ssRMSs have shown heterogeneous enhancement. These findings are similar to

those of the other subtypes of RMS (37). Intratumoral hemorrhages and necrotic changes are occasionally seen in ssRMSs, as in the other subtypes (37).

The minimum ADC of the tumor in the present case was slightly higher than those of the other subtypes of RMS ($0.88 \times 10^{-3} \text{ mm}^2/\text{s}$ versus $0.72 \times 10^{-3} \text{ mm}^2/\text{s}$) (38), and we speculate that this is because the cell density of ssRMS is lower than that of the other subtypes due to the rich fibrocollagenous stroma characterizing

Table 1. Radiological findings of ssRMSs.

Case no.	Age (years)/Sex	Location	T2W imaging	T1W imaging	Contrast enhancement	Hemorrhage	Necrosis	Reference
1	66/F	Tongue	ND	ND	ND	ND	ND	(10)
2	19/M	Tibia	High	Iso	Heterogeneous well	(+)	(+)	(14)
3	23/M	Plantar	High	ND	ND	ND	ND	(21)
4	40/M	Masticator space	High	Iso	ND	ND	ND	(22)
5	40/M	Masticator space	High	ND	ND	ND	(+)	(23)
6	26/F	Chest wall	ND	ND	ND	ND	ND	(24)
7	58/M	Hypopharynx	High	Iso	Well	ND	ND	(27)
8	36/M	Parotid gland	ND	ND	(+)	ND	ND	(28)
9	24/M	Occipital bone	ND	Low	Inconspicuous	ND	(+)	(30)
10	50/M	Hard palate	ND	ND	Heterogeneous	ND	ND	(34)
11	67/F	Masticator space	High	Iso	Heterogeneous well	(+)	(+)	Present case

ssRMSs, spindle cell/sclerosing rhabdomyosarcomas; ND, not described.

the histopathology of ssRMS. The tumor in the present case showed many flow voids on T2W images and elevated blood flow and blood volume on perfusion images, suggesting its hypervascular nature.

In conclusion, we have reported the case of an elderly woman with ssRMS with both extracranial and intracranial components. ssRMSs of the masticator space can show intracranial invasion, which may be associated with a bad prognosis. ssRMSs can grow without bone destruction, which could be a key to differentiate ssRMSs from the conventional subtypes of RMS.

Declaration of conflicting interests

The author(s) declared no potential conflicts of interest with respect to the research, authorship, and/or publication of this article.

Funding

The authors disclosed receipt of the following financial support for the research, authorship, and/or publication of this article: This work was supported by JSPS KAKENHI Grant Number JP17K10410.

References

- Freling NJM, Merks JHM, Saeed P, et al. Imaging findings in craniofacial childhood rhabdomyosarcoma. *Pediatr Radiol* 2010;40:1723–1738.
- Miller RW, Young JL Jr, Novakovic B. Childhood cancer. *Cancer* 1995;75:395–405.
- Weiss S, Goldblum JR. Rhabdomyosarcoma. In: Weiss S, Goldblum JR, eds. *Enzinger and Weiss's soft tissue tumors*. St. Louis, MO: Mosby, 2001:785–835.
- Nascimento AF, Barr FG. Spindle cell/sclerosing rhabdomyosarcoma. In: Fletcher CDM, Bridge JA, Hogendoorn PCW, et al., eds. *WHO Classification of Tumours of Soft Tissue and Bone*. 4th ed. Lyon: IARC, 1993:134–135.
- Mentzel T, Katenkamp D. Sclerosing, pseudovascular rhabdomyosarcoma in adults. *Virchows Arch* 2000;436:305–311.
- Folpe AL, McKenney JK, Bridge JA, et al. Sclerosing rhabdomyosarcoma in adults: report of four cases of a hyalinizing, matrix-rich variant of rhabdomyosarcoma that may be confused with osteosarcoma, chondrosarcoma, or angiosarcoma. *Am J Surg Pathol* 2002;26:1175–1183.
- Vadgama B, Sebire NJ, Malone M, et al. Sclerosing rhabdomyosarcoma in childhood: case report and review of the literature. *Pediatr Dev Pathol* 2004;7:391–396.
- Chiles MC, Parham DM, Qualman SJ, et al. Sclerosing rhabdomyosarcomas in children and adolescents: a clinicopathologic review of 13 cases from the Intergroup Rhabdomyosarcoma Study Group and Children's Oncology Group. *Pediatr Dev Pathol* 2004;7:583–594.
- Croes R, Debiec-Rychter M, Cokelaere K, et al. Adult sclerosing rhabdomyosarcoma: cytogenetic link with embryonal rhabdomyosarcoma. *Virchows Arch* 2005;446:64–67.
- Knipe TA, Chandra RK, Bugg MF. Sclerosing rhabdomyosarcoma: a rare variant with predilection for the head and neck. *Laryngoscope* 2005;115:48–50.
- Kuhnen C, Herter P, Leuschner I, et al. Sclerosing pseudovascular rhabdomyosarcoma—immunohistochemical, ultrastructural, and genetic findings indicating a distinct subtype of rhabdomyosarcoma. *Virchows Arch* 2006;449:572–578.
- Mentzel T, Kuhnen C. Spindle cell rhabdomyosarcoma in adults: clinicopathological and immunohistochemical analysis of seven new cases. *Virchows Arch* 2006;449:554–560.
- Zambrano E, Perez-Atayde AR, Ahrens W, et al. Pediatric sclerosing rhabdomyosarcoma. *Int J Surg Pathol* 2006;14:193–199.
- Sakayama K, Tauchi H, Sugawara Y, et al. A complete remission of sclerosing rhabdomyosarcoma with multiple lung and bone metastases treated with multi-agent

- chemotherapy and peripheral blood stem cell transplantation (PBSCT): a case report. *Anticancer Res* 2008;28:2361–2367.
15. Wang J, Tu X, Sheng W. Sclerosing rhabdomyosarcoma: a clinicopathologic and immunohistochemical study of five cases. *Am J Clin Pathol* 2008;129:410–415.
 16. Bouron-Dal Soglio D, Rougemont A-L, Absi R, et al. SNP genotyping of a sclerosing rhabdomyosarcoma: reveals highly aneuploid profile and a specific MDM2/HMGA2 amplification. *Hum Pathol* 2009;40:1347–1352.
 17. Lamovec J, Volavšek M. Sclerosing rhabdomyosarcoma of the parotid gland in an adult. *Ann Diagn Pathol* 2009;13:334–338.
 18. Gavino ACP, Spears MD, Peng Y. Sclerosing spindle cell rhabdomyosarcoma in an adult: report of a new case and review of the literature. *Int J Surg Pathol* 2010;18:394–397.
 19. Martorell M, Ortiz CM, Garcia JA. Testicular fusocellular rhabdomyosarcoma as a metastasis of elbow sclerosing rhabdomyosarcoma: a clinicopathologic, immunohistochemical and molecular study of one case. *Diagn Pathol* 2010;5:52.
 20. Cantley RL, Cimbalk D, Reddy V, et al. Fine-needle aspiration diagnosis of a metastatic adult sclerosing rhabdomyosarcoma in a lymph node. *Diagn Cytopathol* 2010;38:761–764.
 21. Kikuchi K, Wettach GR, Ryan CW, et al. MDM2 amplification and PI3KCA mutation in a case of sclerosing rhabdomyosarcoma. *Sarcoma* 2013;2013:1–8.
 22. Robinson JC, Richardson MS, Neville BW, et al. Sclerosing rhabdomyosarcoma: report of a case arising in the head and neck of an adult and review of the literature. *Head Neck Pathol* 2013;7:193–202.
 23. Lin X-Y, Wang Y, Yu J-H, et al. Sclerosing rhabdomyosarcoma presenting in the masseter muscle: a case report. *Diagn Pathol* 2013;8:18.
 24. Mikubo M, Ikeda S, Hoshino T, et al. Sclerosing rhabdomyosarcoma of a chest wall in an adult: a case report and review of the literature. *Ann Thorac Cardiovasc Surg* 2014;20:642–645.
 25. Rekhvi B, Singhvi T. Histopathological, immunohistochemical and molecular cytogenetic analysis of 21 spindle cell/sclerosing rhabdomyosarcomas. *APMIS* 2014;122:1144–1152.
 26. Agaram NP, Chen C-L, Zhang L, et al. Recurrent MYOD1 mutations in pediatric and adult sclerosing and spindle cell rhabdomyosarcomas: evidence for a common pathogenesis: MYOD1 mutation in rhabdomyosarcoma. *Genes Chromosomes Cancer* 2014;53:779–787.
 27. Wu T-T, Wang Q-Y, Zhou S-H, et al. Spindle cell rhabdomyosarcoma in the hypopharynx of an adult. *Int J Clin Exp Pathol* 2014;7:5254–5258.
 28. Warner BM, Griffith CC, Taylor WD, et al. Sclerosing rhabdomyosarcoma: presentation of a rare sarcoma mimicking myoepithelial carcinoma of the parotid gland and review of the literature. *Head Neck Pathol* 2015;9:147–152.
 29. Zheng Y, Liu X, Mao Y, et al. Sclerosing rhabdomyosarcoma presenting on the knee-joint. *Indian J Pathol Microbiol* 2015;58:335–337.
 30. Chen Q, Lu W, Li B. Primary sclerosing rhabdomyosarcoma of the scalp and skull: report of a case and review of literature. *Int J Clin Exp Pathol* 2015;8:2205–2207.
 31. Zhao Z, Yin Y, Zhang J, et al. Spindle cell/sclerosing rhabdomyosarcoma: case series from a single institution emphasizing morphology, immunohistochemistry and follow-up. *Int J Clin Exp Pathol* 2015;8:13814–13820.
 32. Yasui N, Yoshida A, Kawamoto H, et al. Clinicopathologic analysis of spindle cell/sclerosing rhabdomyosarcoma: spindle cell/sclerosing RMS. *Pediatr Blood Cancer* 2015;62:1011–1016.
 33. Alaggio R, Zhang L, Sung Y-S, et al. A molecular study of pediatric spindle and sclerosing rhabdomyosarcoma: identification of novel and recurrent VGLL2-related fusions in infantile cases. *Am J Surg Pathol* 2016;40:224–235.
 34. Moran N, Bhuyan UT, Gogoi G, et al. Giant sclerosing oral rhabdomyosarcoma—a unique case. *Indian J Otolaryngol Head Neck Surg* 2016;68:384–386.
 35. Owosho AA, Huang S-C, Chen S, et al. A clinicopathologic study of head and neck rhabdomyosarcomas showing FOXO1 fusion-positive alveolar and MYOD1-mutant sclerosing are associated with unfavorable outcome. *Oral Oncol* 2016;61:89–97.
 36. Lee JH, Lee MS, Lee BH, et al. Rhabdomyosarcoma of the head and neck in adults: MR and CT findings. *Am J Neuroradiol* 1996;17:1923–1928.
 37. Allen SD, Moskovic EC, Fisher C, et al. Adult rhabdomyosarcoma: cross-sectional imaging findings including histopathologic correlation. *Am J Roentgenol* 2007;189:371–377.
 38. Sepahdari AR, Politi LS, Aakalu VK, et al. Diffusion-weighted imaging of orbital masses: multi-institutional data support a 2-ADC threshold model to categorize lesions as benign, malignant, or indeterminate. *Am J Neuroradiol* 2014;35:170–175.